GEOLOGY

Intraplate volcanism triggered by bursts in slab flux

Ben R. Mather[1,2]*, R. Dietmar Müller[1], Maria Seton[1], Saskia Ruttor[3], Oliver Nebel[3], Nick Mortimer[4]

Long-lived, widespread intraplate volcanism without age progression is one of the most controversial features of plate tectonics. Previously proposed edge-driven convection, asthenospheric shear, and lithospheric detachment fail to explain the ~5000-km-wide intraplate volcanic province from eastern Australia to Zealandia. We model the subducted slab volume over 100 million years and find that slab flux drives volcanic eruption frequency, indicating stimulation of an enriched mantle transition zone reservoir. Volcanic isotope geochemistry allows us to distinguish a high-μ (HIMU) reservoir [>1 billion years (Ga) old] in the slab-poor south, from a northern EM1/EM2 reservoir, reflecting a more recent voluminous influx of oceanic lithosphere into the mantle transition zone. We provide a unified theory linking plate boundary and slab volume reconstructions to upper mantle reservoirs and intraplate volcano geochemistry.

INTRODUCTION

Upper mantle fertility is often regarded as a key requirement to trigger intraplate volcanism, particularly in provinces without apparent age progression along volcanic chains (*1*, *2*). Chemical heterogeneities associated with fertility in the mantle are typically introduced by recycling oceanic lithosphere through subduction, which transports volatiles into the mantle (*3*). Recent geodynamic models have been used to infer edge-driven convection as a mechanism to drive upwellings from a dormant volatile-rich mantle reservoir (*4*). Convective cells can form at the trailing edge of lithospheric boundaries and may produce regional volcanism without age progression (*2*). This mantle flow can offer a viable mechanism for focused intraplate volcanism. Elsewhere, deeper hydrous mantle domains associated with active subduction are advocated as the cause for volcanism (*5*). Alternatively, high rates of asthenospheric shear may induce melting and upwelling of low-viscosity pockets of asthenospheric mantle to drive volcanism (*1*). These mechanisms have been used to explain volcanic provinces that have formed in the last 5 million years (Ma), but whether these convective upwellings can be sustained over a longer history of volcanism remains unclear. The eastern third of Australia and the mainly submerged continent of Zealandia have been prone to volcanism since the final stages of eastern Gondwana breakup (*6*). As this 5000-km-wide region migrated northward, it passed over mantle upwellings that produced three distinct chains of hot spot volcanoes: (i) the leucitite-bearing Cosgrove Track (*7*), (ii) the Tasmantid Seamount Chain (*8*), and (iii) the Lord Howe Seamount Chain (*9*). However, there are abundant Cenozoic volcanics in this region without age progression (Fig. 1A). Volcanism is pervasive across continental and oceanic regions; however, the number of samples is not uniformly distributed. Binning regional volcanic products for area and time of eruption reveals that onshore and offshore lava field volcanoes outnumber age-progressive central and leucitite-bearing volcanic eruption products considerably (Fig. 1B; refer to Materials and Methods for binning of eruption ages and locations). Two gradual increases in volcanism occurred between 60 and 21 Ma and between 10 and 2 Ma and were separated by a brief lull in eruption frequency. The latter peak at 2 Ma has been alternatively attributed to edge-driven convection to produce the Newer Volcanics Province along the southeastern margin of Australia (*2*) or asthenospheric shear for volcanic provinces in eastern Australia (*1*), but the majority of volcanism occurs far beyond the boundaries of lithospheric step changes, and high rates of asthenospheric shear are not predicted across the entire 5000-km-wide volcanic province. Lithospheric detachment has been proposed for some volcanism in southern Zealandia (*10*), but it is not clear whether this process can be applied to the entire 5000-km-wide volcanic province. All of these mechanisms rely on regional lithospheric architecture to drive convective upwellings that produce volcanism. However, while these geodynamic models may explain local volcanism, they cannot explain the enigmatic time-space relationships of intraplate volcanism observed in eastern Australia and Zealandia. The chemical signatures of lavas that inherit their unique isotope code from the refertilized mantle heterogeneity offer clues into the melting processes driving volcanism. Recent isotope geochemistry analyses of Sr, Nd, and Pb suggest the Zealandia-Antarctic mantle domain is distinct from Indian and Pacific signatures attributed to mixing of a deep mantle upwelling with a heterogeneous upper mantle (*11*) but with some uncertainty over whether it continues northward into the east Australian–Zealandia region (*12*). Here, using a tectonic plate reconstruction over the last 100 Ma and geochemical analyses of eruption products, we investigated the extent to which the recycling of the Pacific seafloor at subduction zones contributes to increases in widespread volcanism in the entire eastern Australia and Zealandia region.

RESULTS

Numerical models of subduction in the western Pacific exhibit flat subduction due to the thermal buoyancy of the downgoing slab, which leads to slab stagnation in the transition zone (*13*). To quantify the amount of recycled oceanic lithosphere that has entered the transition zone beneath eastern Australia and Zealandia, we calculated the volumetric rate of material consumed at subduction zones (termed "slab flux" in km^3/year) integrated over the last 100 Ma. The convergence rates of downgoing slabs are calculated using global plate reconstruction models (*14*) with the open source GPlates software (www.gplates.org). The geometries of plate boundaries continuously evolve in response to plate motions on the surface of the

[1]EarthByte Group, School of Geoscience, The University of Sydney, Sydney, NSW 2006, Australia. [2]Sydney Informatics Hub, The University of Sydney, Sydney, NSW 2006, Australia. [3]School of Earth, Atmosphere and Environment, Monash University, Clayton, VIC 3800, Australia. [4]GNS Science, Dunedin, New Zealand.
*Corresponding author. Email: ben.mather@sydney.edu.au

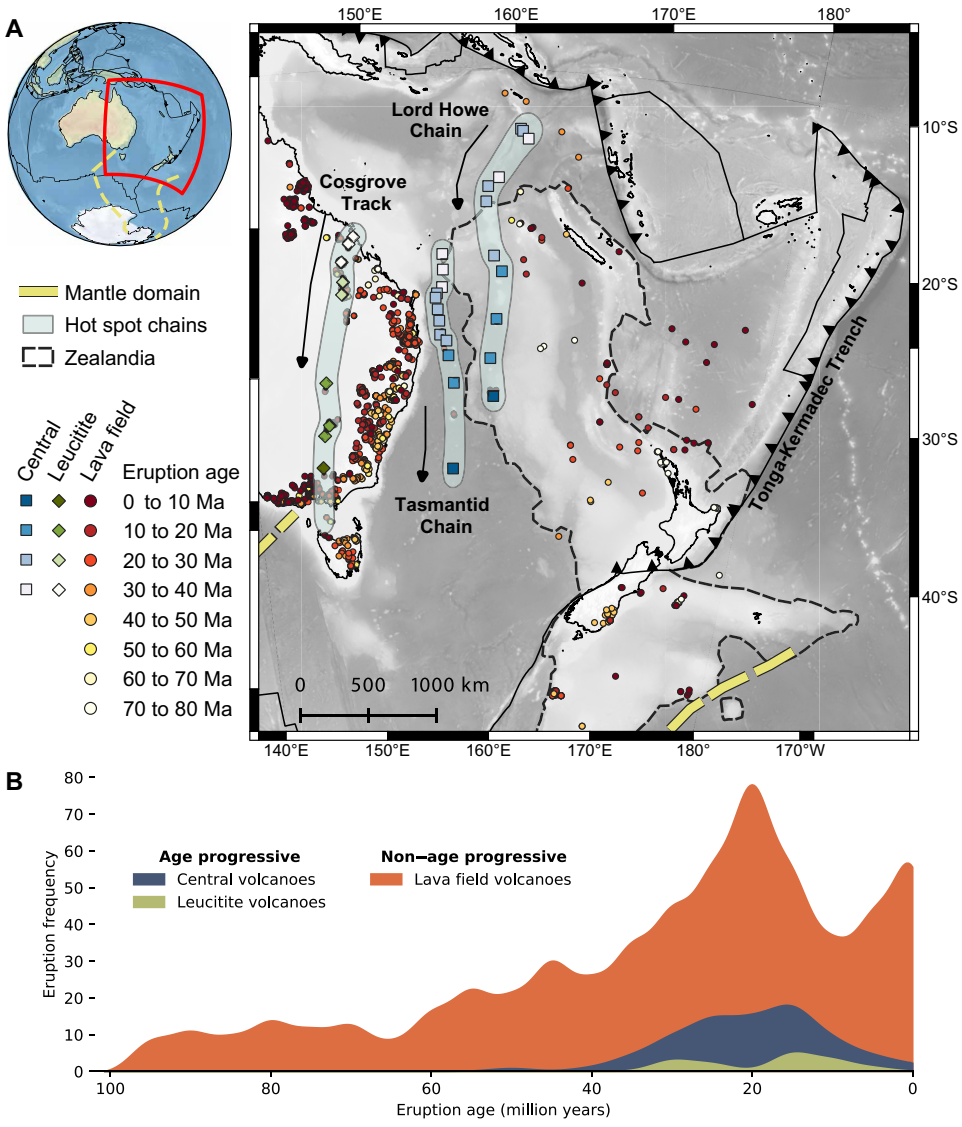

Fig. 1. Map of volcanism in the Australia-Zealandia domain. (**A**) Bathymetric map with major plate boundaries and submarine continental lithosphere, overlain with eruptions colored by eruption age (*6*). The yellow dashed line indicates the extent of the Zealandia-Antarctic domain (*11*). (**B**) Distribution of eruption ages for age-progressive volcanism (central, leucitite-bearing volcanoes) and non–age-progressive volcanism (lava field volcanoes). These data have been consolidated into 1°×1° windows and 5-Ma bins to reduce sample bias (refer to Materials and Methods and fig. S1).

globe. To calculate the volume of oceanic lithosphere passing through a subduction zone, the thickness of the plate must be estimated. Numerous models describe a thickening of oceanic lithosphere as proportional to the square root of thermal diffusivity and age of the seafloor, until a maximum thickness is reached. Here, we use a plate model of lithospheric cooling with a plate thickness of 125 km and mantle potential temperature set to 1350°C (*15*). Using this model calibration, we find the thickness of the oceanic lithosphere from seafloor age grids (*14*) and integrate across the subduction boundary at 1-Ma time intervals to calculate slab flux.

Reconstruction of subducted slab volume

The entire region has accumulated thick piles of Pacific seafloor ingested by subduction zones across the western Pacific (Fig. 2). It is demonstrated here that the eruption frequency of lava field volcanoes gradually increases from 60 to 21 Ma and correlates with an increase in regional slab flux from 20 to 70 km^3/year accommodated by eastward rollback of the subduction boundary while east Australia and Zealandia migrate over thick piles of subducted slabs (Fig. 2A). This 35-Ma period of increasing slab flux was terminated at the collision of the Ontong Java Plateau (OJP) with the Melanesian trench at ~26 Ma (Fig. 2B) (*16*). Following a rapid slowdown of the Australian plate associated with the collision, accompanied by a 50% drop in the eruption frequency of lava field volcanoes after 21 Ma, the northward migration of the Australian plate stabilized at 6.8 cm/year after subduction reestablished along the Trobriand Trough (*16*). A second increase in eruption frequency between 10 and 2 Ma corresponds to an increase in slab flux associated with an acceleration in the northward migration of Australia from 6.8 to 7.5 cm/year (Fig. 2C). Much of the volcanism observed during this period

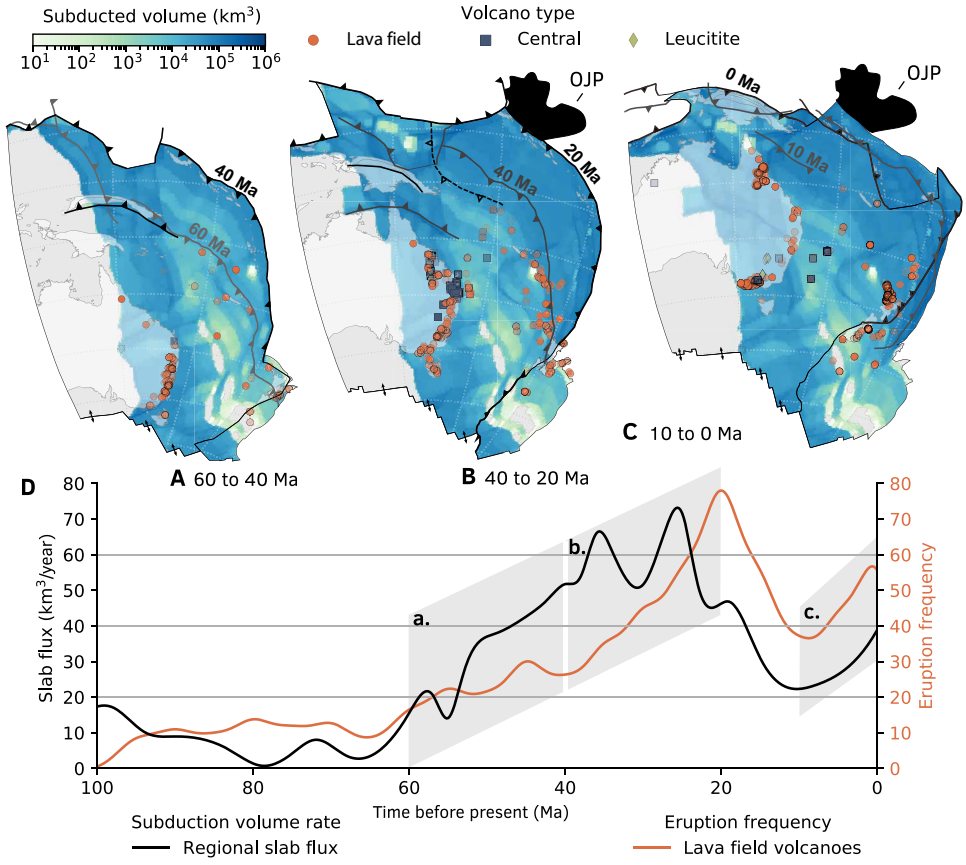

Fig. 2. Cumulative volume of subducted oceanic lithosphere in the western Pacific. Snapshots of the 100-Ma time series were interrogated with the pyGPlates software (www.gplates.org) using a tectonic plate reconstruction (*14*) that was recently revised in the Pacific Ocean. Refer to movie S1 for an animated reconstruction. Volcanic eruptions are grouped into lava field (red circles), central (blue squares), and leucitite-bearing volcanoes (green diamonds). Three sequences capture the tectonic evolution of the Australia-Zealandia domain as Pacific seafloor is recycled into the mantle between the following: (**A**) 60 to 40 Ma as subduction rollback progresses along the western Pacific margin; (**B**) 40 to 20 Ma as Papua New Guinea amalgamated and subduction rollback along the western Pacific continues until the collision of the Ontong Java Plateau with the Melanesian Trench, which causes subduction to reestablish along the Trobriand Trough; and (**C**) 10 to 0 Ma as Australia and Zealandia migrate northward to its present-day location and the reversal of subduction polarity along the northern margin of Australia. (**D**) Regional slab flux plotted against time, which has been smoothed using a Gaussian filter with an SD of 1 Ma, overlain with the eruption frequency of lava field volcanoes from Fig. 1B.

occurs in western Victoria and northern Queensland. Although volcanism in western Victoria may be partially sourced from the mantle plume associated with the Cosgrove Track, because of their proximity in the Late Miocene (*7*), it is also synonymous with an increase in slab flux of 16 km^3/year and a northward migration of the Australian plate at 7.5 cm/year over thick piles of subducted lithosphere (10^4 to 10^5 km^3). The generation of volcanism during increases in slab flux is anticipated as a large volume of material enters the subduction zone and displaces the mantle to generate return flow (*5*, *17*). These upwellings mobilize mantle from a volatile-enriched transition zone that rises to the surface. Following decompression, the surrounding mantle will destabilize and melt during ascent to generate non–age-progressive volcanism. A similar mantle return flow has also been a proposed vehicle to drive volcanism in northeast China, where upwellings associated with subduction of the Pacific has been hypothesized from seismic tomography and geodynamic models (*5*, *18*).

Comparisons to seismic tomography

While seismic tomography models have proved useful to identify transition zone thickness variations from velocity discontinuities, the offshore Australia-Zealandia domain suffers from poor station coverage, which impedes efforts to resolve consistent features among different models. Despite this shortcoming, several tomography models image slower velocity within the transition zone that is consistent with high degrees of volatile content or partial melt (Fig. 3). The shear wave velocity variation within the mantle transition zone shows that a low-velocity anomaly connects eastern Australia to Zealandia and extends as far south as Antarctica (Fig. 3, B and C). Recent radiogenic isotope analyses point to isotopic heterogeneity in the Zealandia-Antarctic mantle domain (*11*), but with some uncertainty whether it continues north (*12*). From shear wave velocity and reconstructions of subducted slab volume, the anomalous Zealandia-Antarctic mantle domain likely extends across the entire 5000-km-wide intraplate volcanic province from eastern Australia to Zealandia.

Cross sections of P-wave tomography indicate flat subduction in the northern section of the Tonga-Kermadec Trench and steeper subduction angles in the south (Fig. 3A). In the northernmost cross section (A-A′), the transition zone is entirely occupied by the stagnant Pacific slab across the volcanic region and broadly correlates with the magnitude of slab volume calculated from our tectonic

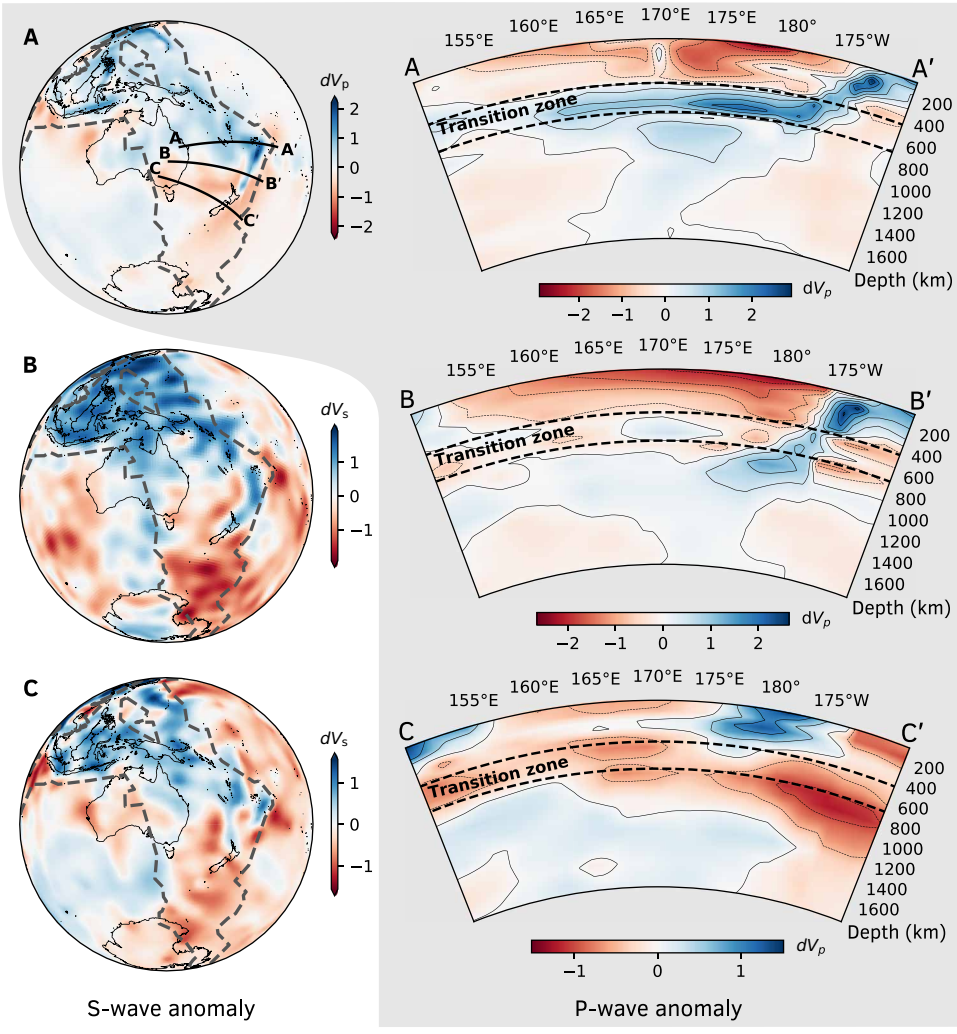

Fig. 3. P- and S-wave velocity variations in the mantle transition zone. The globes of velocity variations in the transition zone are calculated by vertically averaging *dV* from 410 to 660 km and compared across various tomography models: (**A**) TX2019slab P-wave anomaly (*35*) and three accompanying cross sections A-A′, B-B′, and C-C′; (**B**) S40RTS S-wave anomaly (*36*); and (**C**) SL2013SV S-wave anomaly (*37*). The dashed line on each globe indicates the extent of subducted slab material integrated from 120 Ma to the present day (Fig. 2D).

reconstructions (5.5×10^5 km^3). Slab dip is steeper for cross section B-B′ at 33°S, yet pockets of high-velocity anomalies have been resolved west of the subduction zone, which suggests that slab remnants reside in the transition zone beneath Zealandia and the eastern margin of Australia. Cross section C-C′ intersects the South Island of New Zealand and does not resolve any high-velocity anomalies in the transition zone. Here, subduction is congested by the Hikurangi Plateau, thus restricting the volume of oceanic lithosphere entering the mantle. Our map of subducted slab volume lends support to this interpretation of the P-wave velocity anomaly with approximately 10,000 km^3 less oceanic lithosphere having been subducted over the last 60 Ma in this region compared to northern sections of the subduction zone (Fig. 2). The majority of the seafloor that has been subducted since 100 Ma ago will have since sunk deeper into the mantle because of thermal and compositional changes that occur within the slab (*19*). The prevalence of high–P-wave velocity anomalies throughout Zealandia and eastern Australia suggests that the residence time of stagnant slabs varies with latitude along the Tonga-Kermadec Trench. In northern Zealandia, the lateral extent of stagnant slabs in the transition zone suggests a residence time in the order of 60 Ma. This reduces further south as subduction becomes more congested.

Analysis of radiogenic isotope concentration

To test whether the volcanoes in eastern Australia and Zealandia sample fertile source reservoirs in the transition zone, we compiled a comprehensive database of geochemical analyses on volcanic rocks collected within the Australia-Zealandia domain (data files S1 and S2). These data have been filtered to exclude samples that indicate alteration and crustal contamination. Each value exceeding major and trace element ratios indicating alteration has been excluded. For this, we exclude values that have K_2O/P_2O_5 less than 1 (*20*), and MgO lavas less than 4 weight % (wt %) have been excluded because of clinopyroxene, plagioclase, and magnetite fractionation (*21*). All samples have been tested for A-FC (assimilation and fractional crystallization) processes but appear to be not affected, evidenced through the absence of covariations of radiogenic isotopes with indices of

differentiation (MgO and Nb/Sc). Note that applying an even more stringent filter with using only the most primitive samples with MgO > 8 wt % yields a similar trend in all isotope systematics. Nonetheless, four samples show remarkably low radiogenic isotopes below the bulk of all samples, with $^{143}Nd/^{144}Nd < 0.5122$, and tending toward continental crust signatures. Even though there is no clear indication for contamination, these values have been excluded from our interpretation in a conservative approach to exclude any potential bias.

We compared the variation in isotope ratios across the eastern margin of Australia and Zealandia for lava field volcanoes and include age-progressive and, thus, putative plume-related central volcanoes and leucitite suites for comparison (Fig. 4). Above any categorical sorting by volcano type, the strongest variation in isotopic signature is controlled by latitude in this region. At southern latitudes, the lava field volcanoes show strong similarities with high-μ (HIMU)–type mantle reservoirs, as demonstrated by the highly radiogenic $^{206}Pb/^{204}Pb$ and $^{208}Pb/^{204}Pb$, whereas at northern latitudes, these data reflect compositions closer to enriched mantle (EM1/EM2) end-members due to higher $^{87}Sr/^{86}Sr$ (*20*). Elevated $^{87}Sr/^{86}Sr$ in northeastern Australia, for example, is consistent with slab-derived fluids

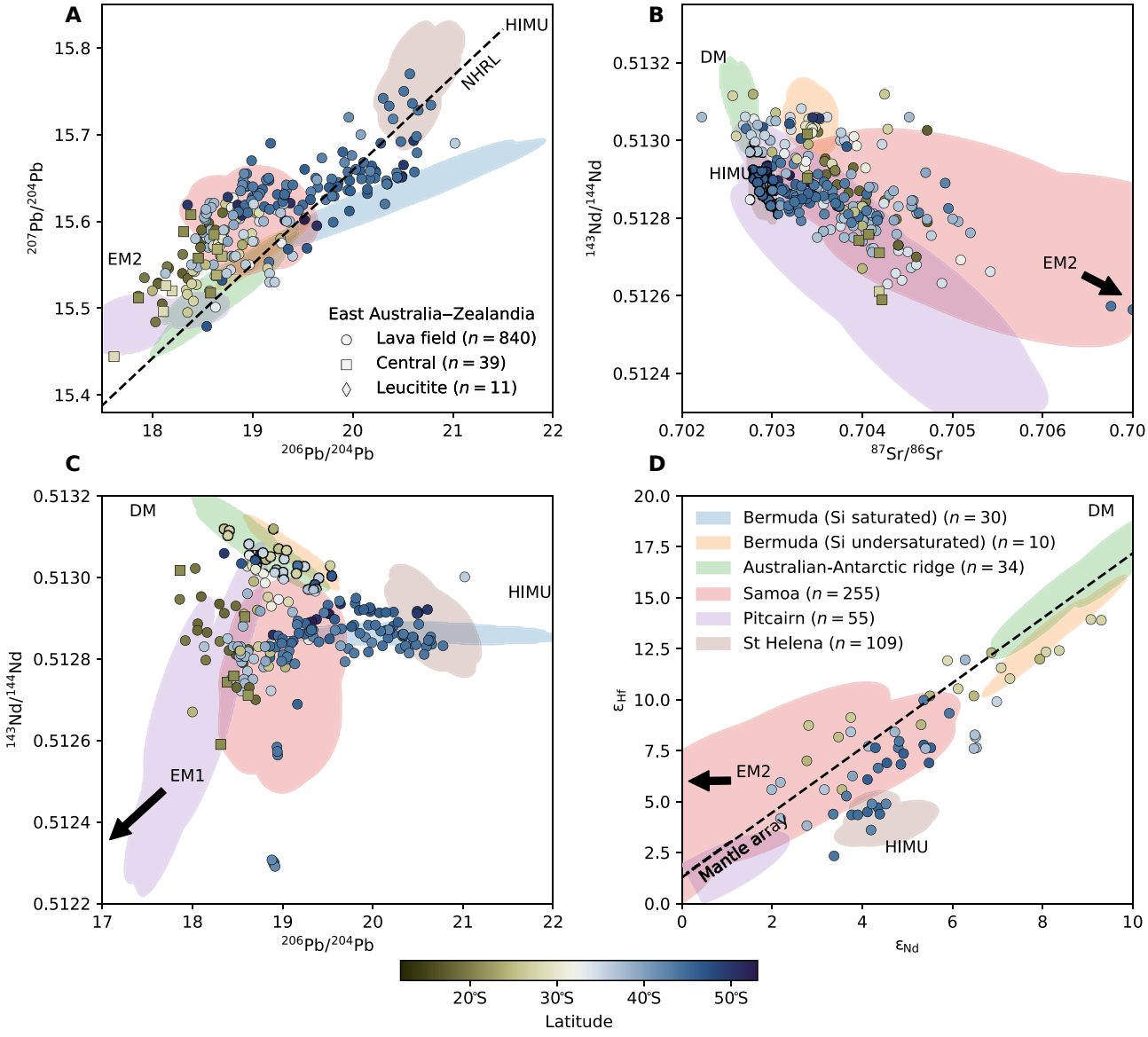

Fig. 4. Radiogenic isotope geochemistry of the Australia-Zealandia domain. Pb, Sr, Nd, and Hf isotopes sorted into lava field, central, and leucitite-bearing volcanoes, all of which are colored by latitude (refer to Fig. 5 for the geographic location of samples used in this analysis). These samples are compared with other intraplate volcanic regions (Bermuda and Canary Islands) and the Australian-Antarctic discordance (*11*). The PETLAB database of geochemical analysis on Zealandia was supplemented by the GEOROC database for East Australian volcanics and to compare with other locations. DM, depleted mantle; EM1, enriched mantle 1; EM2, enriched mantle 2; HIMU, high-μ. (**A**) $^{207}Pb/^{204}Pb$ plotted against $^{206}Pb/^{204}Pb$ superimposed on the Northern Hemisphere Reference Line (NHRL), showing more radiogenic Pb in higher latitudes. (**B**) $^{143}Nd/^{144}Nd$ plotted against $^{87}Sr/^{86}Sr$, showing a higher concentration of $^{87}Sr/^{86}Sr$ and lower concentration of $^{143}Nd/^{144}Nd$ for higher latitudes akin to an EM2 mantle reservoir. (**C**) $^{143}Nd/^{144}Nd$ plotted against $^{206}Pb/^{204}Pb$ showing low $^{143}Nd/^{144}Nd$ for central volcanoes at lower latitudes representing a more EM1 mantle reservoir. (**D**) ε_{Hf} plotted against ε_{Nd} showing the majority of samples plotting close to the mantle array (*38*).

that have been released from subducted slabs to be likely stored in the form of pyroxenitic assemblages in the mantle (*22*, *23*). For southern latitudes, $^{87}Sr/^{86}Sr$ is substantially less radiogenic and more consistent with mixing of an enriched component akin to HIMU. Combined northern $^{176}Hf/^{177}Hf$–$^{143}Nd/^{144}Nd$ plots closer to the mantle array as is expected for EM1/EM2-type melts, while southern lava field volcanoes have low ε_{Hf}-ε_{Nd} analogous to a Proterozoic-Archean age HIMU component (where ε_{Nd} and ε_{Hf} are chondrite-normalized $^{143}Nd/^{144}Nd$ and $^{176}Hf/^{177}Hf$ ratios) (*24*). The gradation of these isotopic domains with north-south dichotomy confirms that mantle heterogeneity in the Zealandia-Antarctic region continues north. Furthermore, seemingly disjointed volcanic fields sample a common source over thousands of kilometers. Melt contamination from lithospheric sources is unlikely to be pervasive over such a large region. We propose that these signatures are related to thick piles of subducted material, which have entered and mixed fluids into the mantle over a prolonged period of time. Similar isotopic signatures have been identified in Bermuda (*3*) and Northeast China (*25*), where volcanoes in these locations have been inferred to sample a fertile mantle inherited from past subduction from the transition zone.

DISCUSSION

From radiogenic isotope analysis, we determine that the volcanic centers in eastern Australia and Zealandia sample recycled oceanic material stored in the transition zone. This is the most plausible locus for the storage of devolatilized material in the mantle, where slabs undergo phase transition, and has been proposed to host EM1 (*5*) or HIMU (*3*, *24*, *26*) signatures. Accordingly, the stimulation of the transition zone by varying rates of subduction throughout the Cenozoic has produced volcanism that sample two distinct mantle reservoirs: EM1/EM2 in the north of the east Australia–Zealandia domain, and HIMU in the south. The partition between these end-members is clearly represented in lava field volcanics at ~33°S (Fig. 5) and is also exhibited in eruption products from central volcanoes, which suggests that they both sample common source components (*27*). It is widely held that in ocean island basalts, HIMU is found in plumes located near the tropics (*28*). Here, however, we extend the HIMU signatures to the far south with isotopic signatures akin to HIMU mantle reservoirs elsewhere that must be derived from a Proterozoic-Archean source to allow for radiogenic ingrowth in Hf-Nd-Pb isotope systematics (*24*, *29*). The mixing between HIMU and EM1/EM2 end-members is a direct consequence of the location at which subducted Pacific seafloor stimulates fluids in the mantle transition zone. Subduction north or south of the partition line controls the proportion of volcanic products that sample distinct EM1/EM2 or HIMU mantle reservoirs, respectively (Fig. 6). The transition to EM1/EM2 in the north is likely caused by dehydration or melting of oceanic crust as it is recycled into the mantle or during the return of crustal material in ascending mantle plumes (*30*). Either process would store pyroxenite within the mantle transition zone, obtained from melting of metabasalt (Si undersaturated) or sediment (Si saturated) in subducted seafloor (*23*). The critical mechanism for these components to rise to the surface is the stimulation

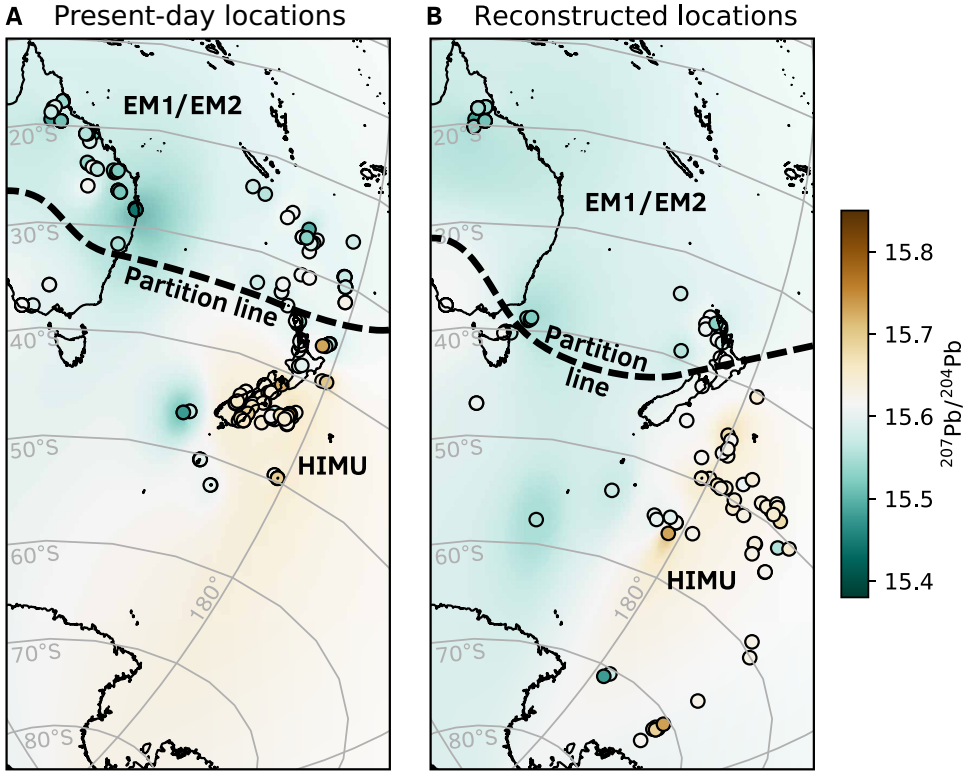

Fig. 5. Geographic partitioning of isotopic domains. The circles represent the geographic locations of geochemical samples at (**A**) the present day, where the partition between dominantly HIMU and EM1/EM2 isotope signature occurs at approximately 33°S, and (**B**) their eruption age (for those data that have recorded ages), which shifts the partition line south to ~38°S. If the composition of the mantle transition zone has not evolved significantly since the eruption time, then (B) represents the current isotopic partitioning beneath the tectonic plates.

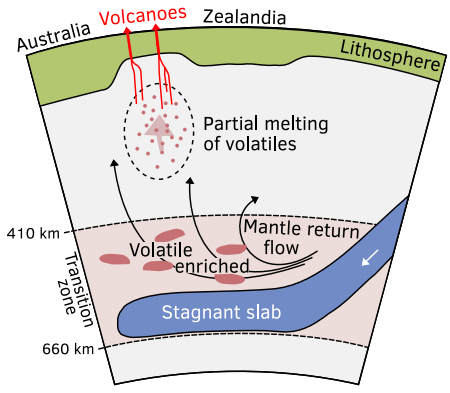

Fig. 6. Conceptual geodynamic model of intraplate volcanism. Perturbation of the transition zone by subducted slabs mobilizes mantle from a volatile-enriched transition zone that rise to the surface. Following decompression, the surrounding mantle will destabilize and melt during ascent to generate non–age-progressive volcanism. Increases in slab flux encourage more vigorous mantle upwelling, which enhances the frequency of volcanic eruptions.

of the mantle transition zone by subducting slabs. The EM1/EM2 signature is likely emphasized here because a higher volume of oceanic lithosphere has been recycled in northern Zealandia in the last 100 Ma compared to the south. Relatively unimpeded subduction in the northern segment of the trench supplies a higher flux of volatile-rich sediments and crust into the transition zone that stimulates a mantle reservoir imbued with an EM1/EM2 signature.

Recycled materials stored in the transition zone can be liberated by upwellings associated with slab flux. Volcanic eruptions become more frequent with higher rates of slab flux due to the displacement of an existing enriched reservoir in the transition zone by newly entered subducted slabs. This starts a domino effect that links concurrent slab flux with volcanism, which samples ancient mantle reservoirs. In the case of the east Australia–Zealandia, this represents the mechanism driving increases in volcanism between 60 and 20 Ma and between 10 and 2 Ma, which were previously unexplained. There are, however, many intraplate regions underlain by subducted slabs that are not volcanically active. What sets the east Australia–Zealandia domain apart is that the Jurassic-Cretaceous seafloor that has been subducted in the western Pacific from 60 to 10 Ma ago is imbued with a high concentration of carbon with high U/Pb and hydrous minerals in the crust (*31*). The hot house climate that persisted throughout the Jurassic and Cretaceous accelerated hydrothermal circulation in oceanic crust to increase carbon uptake (*32*, *33*). The flat subduction of carbonated seafloor would likely promote dehydration reactions in the slab that infuse the mantle transition zone. A similar process would have operated in the past to forge a widespread, volatile-rich transition zone, which, with time, evolves into an HIMU reservoir (*34*). It seems most plausible that the shallow subduction of the Pacific plate caused an upward movement of this material and its partial melting, evidenced by the temporal connection between slab flux and volcanic activity. From the temporal relationship in Fig. 2, it becomes apparent that this may incur a lag or delay in response in upwelling of up to 3 Ma. If the entrainment of ancient volatiles in upwelling mantle is linked to flat subduction, then the mechanism driving volcanism we have identified for east Australia–Zealandia may be applied to other intraplate regions globally. For example, a similar mechanism for intraplate volcanism has been proposed for eastern China, whereby subducting slabs have triggered upwellings from a hydrous mantle transition zone (*5*). Cenozoic eruption products there sample a dominantly EM1 component (*25*), which is consistent with the composition of non–age-progressive volcanics in eastern Australia and Zealandia, where there is high slab flux. While the proposed model in eastern China has been applied to the entire Cenozoic era, our reconstructions of slab flux may help refine the temporal and spatial distribution of eruptions across multiple provinces. Similar mechanisms are also relevant for volcanism in the Western United States, which occurs sufficiently far from the plate boundary to be considered intraplate, and in Bermuda (*3*), which also samples an enriched mantle transition zone consistent with past subduction.

MATERIALS AND METHODS

Binning of eruption ages in east Australia and Zealandia

The database of volcanic eruption ages from east Australia and Zealandia was consolidated into 1° × 1° windows and 5-Ma bins to facilitate the analysis of eruption frequency in Fig 2E. The database contains duplicate measurements on the same volcano, which bias the regional distribution of eruptions. Furthermore, the distribution of samples is concentrated on continental settings, and few points have been measured on the seafloor. To address these issues, the region was binned into 1° × 1° windows to consolidate multiple samples that occur in the same location and better represent the distribution of volcanism across the region. In addition, multiple samples that were dated to approximately the same time should represent a single eruption event, which is why the timing of eruptions is consolidated into 5-Ma bins. Varying the spatial or temporal binning results in very little difference to the shape of the eruption frequency distribution for lava field, central, or leucitite volcanoes (fig. S1).

SUPPLEMENTARY MATERIALS

Supplementary material for this article is available at http://advances.sciencemag.org/cgi/content/full/6/51/eabd0953/DC1

REFERENCES AND NOTES

1. C. P. Conrad, T. A. Bianco, E. I. Smith, P. Wessel, Patterns of intraplate volcanism controlled by asthenospheric shear. *Nat. Geosci.* **4**, 317–321 (2011).
2. D. R. Davies, N. Rawlinson, On the origin of recent intraplate volcanism in Australia. *Geology* **42**, 1031–1034 (2014).
3. S. E. Mazza, E. Gazel, M. Bizimis, R. Moucha, P. Béguelin, E. A. Johnson, R. J. McAleer, A. V. Sobolev, Sampling the volatile-rich transition zone beneath Bermuda. *Nature* **569**, 398–403 (2019).
4. S. D. King, D. L. Anderson, Edge-driven convection. *Earth Planet. Sci. Lett.* **160**, 289–296 (1998).
5. J. Yang, M. Faccenda, Intraplate volcanism originating from upwelling hydrous mantle transition zone. *Nature* **579**, 88–91 (2020).
6. P. M. Vasconcelos, K. M. Knesel, B. E. Cohen, J. A. Heim, Geochronology of the Australian Cenozoic: A history of tectonic and igneous activity, weathering, erosion, and sedimentation. *Aust. J. Earth Sci.* **55**, 865–914 (2008).
7. D. R. Davies, N. Rawlinson, G. Iaffaldano, I. H. Campbell, Lithospheric controls on magma composition along Earth's longest continental hotspot track. *Nature* **525**, 511–514 (2015).
8. I. McDougall, R. A. Duncan, Age progressive volcanism in the Tasmantid Seamounts. *Earth Planet. Sci. Lett.* **89**, 207–220 (1988).
9. M. Seton, S. Williams, N. Mortimer, S. Meffre, S. Micklethwaite, S. Zahirovic, Magma production along the Lord Howe Seamount Chain, northern Zealandia. *Geol. Mag.* **156**, 1605–1617 (2019).
10. K. Hoernle, J. D. L. White, P. van den Bogaard, F. Hauff, D. S. Coombs, R. Werner, C. Timm, D. Garbe-Schönberg, A. Reay, A. F. Cooper, Cenozoic intraplate volcanism on New Zealand: Upwelling induced by lithospheric removal. *Earth Planet. Sci. Lett.* **248**, 350–367 (2006).

11. S.-H. Park, C. H. Langmuir, K. W. W. Sims, J. Blichert-Toft, S.-S. Kim, S. R. Scott, J. Lin, H. Choi, Y.-S. Yang, P. J. Michael, An isotopically distinct Zealandia–Antarctic mantle domain in the Southern Ocean. *Nat. Geosci.* **12**, 206–214 (2019).
12. C. A. Finn, R. D. Müller, K. S. Panter, A Cenozoic diffuse alkaline magmatic province (DAMP) in the southwest Pacific without rift or plume origin. *Geochem. Geophys. Geosyst.* **6**, Q02005 (2005).
13. S. D. King, D. J. Frost, D. C. Rubie, Why cold slabs stagnate in the transition zone. *Geology* **43**, 231–234 (2015).
14. R. D. Müller, M. Seton, S. Zahirovic, S. E. Williams, K. J. Matthews, N. M. Wright, G. E. Shephard, K. T. Maloney, N. Barnett-Moore, M. Hosseinpour, D. J. Bower, J. Cannon, Ocean basin evolution and global-scale plate reorganization events since pangea breakup. *Annu. Rev. Earth Planet. Sci.* **44**, 107–138 (2016).
15. C. J. Grose, Properties of oceanic lithosphere: Revised plate cooling model predictions. *Earth Planet. Sci. Lett.* **333–334**, 250–264 (2012).
16. K. M. Knesel, B. E. Cohen, P. M. Vasconcelos, D. S. Thiede, Rapid change in drift of the Australian plate records collision with Ontong Java plateau. *Nature* **454**, 754–757 (2008).
17. C. Faccenna, T. W. Becker, S. Lallemand, Y. Lagabrielle, F. Funiciello, C. Piromallo, Subduction-triggered magmatic pulses: A new class of plumes? *Earth Planet. Sci. Lett.* **299**, 54–68 (2010).
18. Y. Tang, M. Obayashi, F. Niu, S. P. Grand, Y. J. Chen, H. Kawakatsu, S. Tanaka, J. Ning, J. F. Ni, Changbaishan volcanism in northeast China linked to subduction-induced mantle upwelling. *Nat. Geosci.* **7**, 470–475 (2014).
19. W. Mao, S. Zhong, Slab stagnation due to a reduced viscosity layer beneath the mantle transition zone. *Nat. Geosci.* **11**, 876–881 (2018).
20. A. W. Hofmann, Sampling mantle heterogeneity through oceanic basalts: Isotopes and trace elements. *Treatise Geochem.* **3**, 67–101 (2014).
21. J. M. Rhodes, S. Huang, F. A. Frey, M. Pringle, G. Xu, Compositional diversity of Mauna Kea shield lavas recovered by the Hawaii Scientific Drilling Project: Inferences on source lithology, magma supply, and the role of multiple volcanoes. *Geochem. Geophys. Geosyst.* **13**, Q03014 (2012).
22. S. Y. O'Reilly, M. Zhang, Geochemical characteristics of lava-field basalts from eastern Australia and inferred sources: Connections with the subcontinental lithospheric mantle? *Contrib. Mineral. Petrol.* **121**, 148–170 (1995).
23. C. Spandler, G. Yaxley, D. H. Green, D. Scott, Experimental phase and melting relations of metapelite in the upper mantle: Implications for the petrogenesis of intraplate magmas. *Contrib. Mineral. Petrol.* **160**, 569–589 (2010).
24. O. Nebel, R. J. Arculus, W. van Westrenen, J. D. Woodhead, F. E. Jenner, Y. J. Nebel-Jacobsen, M. Wille, S. M. Eggins, Coupled Hf-Nd-Pb isotope co-variations of HIMU oceanic island basalts from Mangaia, Cook-Austral islands, suggest an Archean source component in the mantle transition zone. *Geochim. Cosmochim. Acta* **112**, 87–101 (2013).
25. X.-J. Wang, L.-H. Chen, A. W. Hofmann, F.-G. Mao, J.-Q. Liu, Y. Zhong, L.-W. Xie, Y.-H. Yang, Mantle transition zone-derived EM1 component beneath NE China: Geochemical evidence from Cenozoic potassic basalts. *Earth Planet. Sci. Lett.* **465**, 16–28 (2017).
26. S. Huang, O. Tschauner, S. Yang, M. Humayun, W. Liu, S. N. Gilbert Corder, H. A. Bechtel, J. Tischler, HIMU geochemical signature originating from the transition zone. *Earth Planet. Sci. Lett.* **542**, 116323 (2020).
27. I. Jones, T. Ubide, T. Crossingham, B. Wilding, C. Verdel, Evidence of a common source component for east Australian Cenozoic mafic magmatism. *Lithos* **354–355**, 105254 (2020).
28. M. G. Jackson, T. W. Becker, J. G. Konter, Geochemistry and distribution of recycled domains in the mantle inferred from Nd and Pb isotopes in oceanic hot spots: Implications for storage in the large low shear wave velocity provinces. *Geochem. Geophys. Geosyst.* **19**, 3496–3519 (2018).
29. R. A. Cabral, M. G. Jackson, E. F. Rose-Koga, K. T. Koga, M. J. Whitehouse, M. A. Antonelli, J. Farquhar, J. M. D. Day, E. H. Hauri, Anomalous sulphur isotopes in plume lavas reveal deep mantle storage of Archaean crust. *Nature* **496**, 490–493 (2013).
30. A. Rosenthal, G. M. Yaxley, D. H. Green, J. Hermann, I. Kovács, C. Spandler, Continuous eclogite melting and variable refertilisation in upwelling heterogeneous mantle. *Sci. Rep.* **4**, 6099 (2014).
31. R. D. Müller, A. Dutkiewicz, Oceanic crustal carbon cycle drives 26-million-year atmospheric carbon dioxide periodicities. *Sci. Adv.* **4**, eaaq0500 (2018).
32. L. A. Coogan, K. M. Gillis, Low-temperature alteration of the seafloor: Impacts on ocean chemistry. *Annu. Rev. Earth Planet. Sci.* **46**, 21–45 (2018).
33. K. Li, L. Li, D. G. Pearson, T. Stachel, Diamond isotope compositions indicate altered igneous oceanic crust dominates deep carbon recycling. *Earth Planet. Sci. Lett.* **516**, 190–201 (2019).
34. Y. Weiss, C. Class, S. L. Goldstein, T. Hanyu, Key new pieces of the HIMU puzzle from olivines and diamond inclusions. *Nature* **537**, 666–670 (2016).
35. C. Lu, S. P. Grand, H. Lai, E. J. Garnero, TX2019slab: A new *P* and *S* tomography model incorporating subducting slabs. *J. Geophys. Res. Solid Earth* **124**, 11549–11567 (2019).
36. J. Ritsema, A. Deuss, H. J. van Heijst, J. H. Woodhouse, S40RTS: A degree-40 shear-velocity model for the mantle from new Rayleigh wave dispersion, teleseismic traveltime and normal-mode splitting function measurements. *Geophys. J. Int.* **184**, 1223–1236 (2011).
37. A. J. Schaeffer, S. Lebedev, Global shear speed structure of the upper mantle and transition zone. *Geophys. J. Int.* **194**, 417–449 (2013).
38. C. Chauvel, E. Lewin, M. Carpentier, N. T. Arndt, J.-C. Marini, Role of recycled oceanic basalt and sediment in generating the Hf-Nd mantle array. *Nat. Geosci.* **1**, 64–67 (2008).
39. R. L. Rudnick, D. M. Fountain, Nature and composition of the continental crust: A lower crustal perspective. *Rev. Geophys.* **33**, 267–309 (1995).
40. A. Gale, C. A. Dalton, C. H. Langmuir, Y. Su, J.-G. Schilling, The mean composition of ocean ridge basalts. *Geochem. Geophys. Geosyst.* **14**, 489–518 (2013).

Acknowledgments

Funding: This study was supported by the NSW Department of Industry and the AuScope Simulation, Analysis & Modelling node funded by the Australian government through the National Collaborative Research Infrastructure Strategy (NCRIS). **Author contributions:** B.R.M. simulated the slab flux along subduction zone segments, compiled the isotope and trace element geochemistry, interpreted the isotope geochemistry, wrote the paper, and prepared the figures and tables. R.D.M. and M.S. conceived the project and prepared the figures. S.R. and O.N. interpreted the trace element geochemistry. N.M. provided the offshore geochemistry database "PETLAB" for Zealandia. **Competing interests:** The authors declare that they have no competing interests. **Data and materials availability:** All data needed to evaluate the conclusions in the paper are present in the paper and/or the Supplementary Materials. Code to reproduce the results is freely available at www.gplates.org/download.html. Additional data related to this paper may be requested from the authors.

Submitted 31 May 2020
Accepted 29 October 2020
Published 16 December 2020
10.1126/sciadv.abd0953

Citation: B. R. Mather, R. D. Müller, M. Seton, S. Ruttor, O. Nebel, N. Mortimer, Intraplate volcanism triggered by bursts in slab flux. *Sci. Adv.* **6**, eabd0953 (2020).